PRAMANA
— journal of
physics

© Printed in India

Vol. 41, No. 3,
September 1993
pp. 239–255

Electronic structure of hydrogen and muonium in Al, Mg and Cu

PAWAN SINGH and S PRAKASH
Department of Physics, Panjab University, Chandigarh 160014, India

MS received 22 March 1993; revised 19 May 1993

Abstract. The electronic structure of hydrogen and muonium in simple metals is investigated. The spherical solid model potential is used for the discrete lattice and the Blatt correction for lattice dilation. The proton and muon are kept at the octahedral sites in the fcc and hcp lattices and self-consistent non-linear screening calculations are carried out. The scattering phase shifts, electronic charge density, effective impurity potential, self-energy, charge transfer, residual resistivity and Knight shift are calculated. The spherical solid potential changes the scattering character of impurity. The phase shifts are found slowly converging. The scattering is more prominent in Al than in Mg and Cu. The virtual bound states of proton and muon are favoured in all the three metals. The calculated value of residual resistivity for CuH is in good agreement with the experimental value. The results for Knight shift for μ^+ in Cu and Mg are in reasonable agreement with the experimental values while those for μ^+ in Al are lower than the experimental value. The analytical expressions for effective impurity potential and electronic charge density are suggested.

Keywords. Hydrogen; muonium; Knight shift; resistivity

PACS Nos 71·50; 71·55

1. Introduction

Hydrogen atoms dissolved in a metal dissociate into protons and electrons. Protons being attractive centre are screened by conduction electrons. The first linear screening theory of proton in Cu was proposed by Friedel [1]. It was realized later that the proton-electron interaction is strong. The screening may not be linear and even the bound state may exist. Popovic *et al* [2] used Hohenberg–Kohn–Sham density functional formalism for the non-linear screening of the proton in the jellium model of the metal. Jena and Singwi [3] added the first gradient correction of exchange-correlation potential and found shallow *s* type bound state of the proton. Manninen and Nieminen [4] added the effect of discrete lattice through spherical solid model of the metal and calculated Knight shift, electric field gradient and heat of solution of hydrogen and muonium in simple metals.

When proton or muon is at an interstitial site it displaces host ions from the equilibrium positions. Therefore the positive charge density in the vicinity of the proton reduces, consequently the effective charge on the proton changes. The lattice dilation also introduces the strain field, therefore the total energy of the system also changes [5–6].

The above studies of non-linear screening of proton and muon are inconclusive because either the discrete lattice effect or the size effect is ignored. We thought it

worthwhile to study the electronic structure of hydrogen and muonium in simple metals including both the effects. The discrete lattice effect and the size effect are included through the spherical solid model of the metal and Blatt correction [4–5] respectively. The self-consistent impurity potential, the induced charge density, charge transfer, residual resistivity and Knight shift are investigated.

The plan of the paper is as follows. The necessary formalism is presented in § 2. Calculations and results are presented in § 3 and are discussed in § 4.

2. Theory

2.1 *Size effect*

The screening cloud of conduction electrons and the zero point motion of proton and muon do not allow them to remain as static point charges. These impurities regain the finite size and displace the host ions away from the equilibrium positions. Therefore the positive charge density decreases and electronic charge density increases in the vicinity of the impurity. This changes the positive charge on the proton and the net protonic charge Z is given as [5]

$$Z = Z_{\mathrm{I}} - \frac{\delta V}{V} Z_{\mathrm{H}} \tag{1}$$

where Z_{I} and Z_{H} are the proton and the host atom ionicities respectively and $(\delta V/V)$ is the fractional change in atomic volume. If $(\delta V/V)$ is negative, Z becomes greater than Z_{I}. In the continuum model of the lattice $(\delta V/V)$ is taken as local dilation around the impurity and is given as

$$\frac{\delta V}{V} = \left(\frac{3}{\gamma_E}\right)\left(\frac{1}{a}\right)\left(\frac{\mathrm{d}a}{\mathrm{d}c}\right) \tag{2}$$

where $\gamma_E = [3(1-\sigma)/(1+\sigma)]$, σ is Poisson ratio, $(1/a)$ $(\mathrm{d}a/\mathrm{d}c)$ is the relative change in the lattice parameter a in per cent per atomic per cent impurity and c is the concentration.

2.2 *Discrete lattice effect and non-linear screening*

We use Hohenberg–Kohn–Sham density functional formalism for non-linear screening [7]. A set of wave functions ψ_i with energy eigenvalues ε_i are generated through one particle Schrödinger equation [4]

$$\left[-\frac{1}{2}\nabla^2 + V(\mathbf{r})\right]\psi_i(\mathbf{r}) = \varepsilon_i \psi_i(\mathbf{r}). \tag{3}$$

The atomic units are used throughout. The first term on the left side is kinetic energy operator and the second term is the effective potential seen by an electron which is given

$$V(\mathbf{r}) = V_c(\mathbf{r}) + V_{xc}(n, \mathbf{r}) + V_{ss}(\mathbf{r}). \tag{4}$$

Here $V_c(\mathbf{r})$ is the electrostatic potential due to impurity induced electronic charge

distribution. Explicitly it is given as

$$V_c(\mathbf{r}) = \int \frac{d\mathbf{r}'[n(\mathbf{r}') - n_+(\mathbf{r}')]}{|\mathbf{r} - \mathbf{r}'|} \tag{5}$$

where

$$n(\mathbf{r}) = \sum_{\varepsilon_i < \mu} |\psi_i(\mathbf{r})|^2 \tag{6}$$

and for an interstitial impurity

$$n_+(\mathbf{r}) = n_0 + Z\delta(\mathbf{r}). \tag{7}$$

Here μ is chemical potential and is taken equal to Fermi energy. The origin is at the impurity site, $n_0 (= 3/4\pi r_s^3)$ is uniform positive charge density of the host and r_s is interelectronic distance.

The second term in (4) is exchange-correlation potential which in the local density approximation is given as [8]

$$V_{xc}(n, \mathbf{r}) \simeq \varepsilon_{xc}(n(r)) + n\left(\frac{d\varepsilon_{xc}}{dn}\right)_{n=n(r)} - V_{xc}(n_0, r_s). \tag{8}$$

The following parametrized form of the exchange-correlation energy $\varepsilon_{xc}(n(r))$ in eq. (8) is used [8]

$$\varepsilon_{xc}(n(r)) = -\frac{0{\cdot}9163}{r_s'} - 0{\cdot}112 + 0{\cdot}0335 \ln r_s' - \frac{0{\cdot}02}{0{\cdot}1 + r_s'}, \tag{9}$$

where $r_s' = [3/(4\pi n(r))]^{1/3}$. The potential $V_{xc}(n_0, r_s)$ in (8) is subtracted for convergence.

$V_{ss}(r)$, the last term of (4), is the spherical solid model potential. It is taken as the spherical average of the difference between the bare ion potential and electrostatic potential of the positive background of jellium. The explicit expression is

$$V_{ss}(\mathbf{r}) = -\frac{1}{4\pi}\int d\Omega \sum_L w(\mathbf{r} - \mathbf{R}_L) + \int \frac{d\mathbf{r}' n_0}{|\mathbf{r} - \mathbf{r}'|} \tag{10}$$

where $w(\mathbf{r})$ is the bare ion potential, $\mathbf{R}_L$ are the position vectors of the host atoms and $d\Omega$ is the elementary solid angle. For simplicity we used Ashcroft model potential for bare ions i.e.

$$w(r) = -\frac{Z_H}{r}\theta(r - r_c) \tag{11}$$

where r_c is potential parameter and $\theta(r)$ is unit step function. $V_{ss}(\mathbf{r})$ accounts for the discrete lattice of the host, however exact lattice symmetry is reduced to spherical symmetry due to angular averaging.

3. Calculation and results

3.1 *Effective charge on the proton and muon*

The effective charges on proton and muon in Al, Mg and Cu metals are estimated using (1) as described by Mahajan and Prakash [5]. The values of $(\delta V/V)$ and Z are given in table 1. The experimental value of $(\delta V/V)$ for hydrogen in Cu is taken from Katz *et al* [9] while for hydrogen in Al it is estimated from the data for hydrogen in Cu, Ni and Pd [10]. $\delta V/V$ for hydrogen in Mg is estimated from the ratio of moduli of rigidity of Al and Mg as both the metals have almost the same packing ratio.

Schilling *et al* [11] pointed out that muon, because of its smaller mass and larger zero point energy, causes 1·3 times more volume expansion than a proton in Cu. Therefore, in the absence of any other information $(\delta V/V)$ for muon in Al, Mg and Cu is obtained by multiplying the corresponding values of $(\delta V/V)$ for hydrogen in these metals by a factor of 1·3. The effective charge reduces by about 40% for proton and 50% for muon in Al and Mg metals. This reduction in charge is only 27% for proton and 35% for muon in Cu.

3.2 *Spherical solid model potential*

The two terms on the right side of (10) are calculated separately. The integral in the second term is separated into two parts: $r < r'$ and $r > r'$. These integrals are evaluated and the boundary condition that the potential vanishes as $r \to \infty$ is used. The detailed calculation gives this contribution as

$$V_1 = \frac{-2\pi n_0}{3} r^2. \tag{12}$$

The contribution of the first term on the right side of (10) is evaluated in the same coordinate system for Ashcroft model potential. This calculation is separated into three parts: the potential at the interstitial site, the potential in the region $|\mathbf{R}_i - \mathbf{r}_c| \leqslant r \leqslant |\mathbf{R}_i + \mathbf{r}_c|$ and $r > |\mathbf{R}_i + \mathbf{r}_c|$. The potential at origin is obtained by Ewald–Fuchs method and is equal to the negative of self-energy of the host ion i.e.

$$V_2 = \frac{Z_H \alpha_{EW}}{R_{WS}} + \sum_i \frac{Z_H}{|\mathbf{R}_i|} \theta(r - R_1 - r_c) \tag{13}$$

where α_{EW} is the Madelung constant for octahedral site in both the fcc and hcp lattices and $R_{WS}(=(Z_H^{1/3})r_s)$ is the Wigner–Sejtz radius. $\mathbf{R}_i$ are the coordinates of host atoms with respect to the octahedral site. The potential at any point r in the Ashcroft sphere of radius r_c around each ion i.e. $|\mathbf{R}_i - \mathbf{r}_c| \leqslant r \leqslant |\mathbf{R}_i + \mathbf{r}_c|$ is

$$V_3 = -\frac{1}{4\pi} \sum_i \int \frac{Z_H}{|\mathbf{r} - \mathbf{R}_i|} d\Omega$$

$$= -\sum_i \frac{Z_H}{2rR_i}(r + R_i - r_c); \quad |\mathbf{R}_i - \mathbf{r}_c| \leqslant r \leqslant |\mathbf{R}_i + \mathbf{r}_c| \tag{14}$$

and the potential outside the Ashcroft sphere i.e. $r > |\mathbf{R} + \mathbf{r}_c|$

$$V_4 = -\sum_i \frac{Z_H}{|\mathbf{r}|}; \quad r > |\mathbf{R}_i + \mathbf{r}_c|. \tag{15}$$

Table 1. The calculated results for $AlH(\mu^+)$, $MgH(\mu^+)$ and $CuH(\mu^+)$. $(\delta V/V)$ is fractional change in atomic volume, Z is effective charge on impurity, β is potential parameter, n_s is net charge on impurity, E_s is self-energy, $\Delta\rho$ is residual resistivity and K is Knight shift.

Physical quantities	AlH	Alμ^+	MgH	Mgμ^+	CuH	Cuμ^+
$\delta V/V$	0·13	0·17	0·21	0·27	0·27	0·35
Z	0·61	0·49	0·58	0·46	0·73	0·65
β	1·22	1·18	1·12	1·07	1·20	1·15
$n_s(e)$	0·46	0·39	0·45	0·37	0·54	0·49
E_s(a.u.)	−0·042	−0·026	−0·035	−0·021	−0·060	−0·045
$\Delta\rho(\mu\Omega$cm/at%) (exp)	—	—	—	—	1·5 ± ·05	—
(cal)	0·20	0·14	0·71	0·52	1·53	1·20
K(ppm) (exp)	—	79·6 ± 4·0	—	43·3 ± 3·5	—	60·3 ± 3·0
(cal)	44·39	33·41	38·01	30·14	54·90	48·24

Adding all the four contributions V_1, V_2, V_3 and V_4 and subtracting the constant potential $V_{ss}(r \to \infty) = 3r_c^2/2r_s^3$ for convergence purpose one finds

$$V_{ss}(r) = V_{ss}(0) - \frac{2\pi n_0 r^3}{3} - \begin{cases} \sum_i \left(\frac{Z_H}{2rR_i}(r + R_i - r_c) - \frac{Z_H}{|\mathbf{R}_i|} \right) & ; \quad |\mathbf{R}_i - \mathbf{r}_c| \leqslant \mathbf{r} \leqslant |\mathbf{R}_i + \mathbf{r}_c| \\ \sum_i \left(\frac{Z_H}{|\mathbf{r}|} - \frac{Z_H}{|\mathbf{R}_i|} \right) & ; \quad r > |\mathbf{R}_i + \mathbf{r}_c| \end{cases} \tag{16}$$

where

$$V_{ss}(0) = \frac{Z_H \alpha_{EW}}{R_{WS}} - \frac{3r_c^2}{2r_s^3}. \tag{17}$$

The potential parameter r_c, Madelung constant α_{EW}, octahedral coordinates and R_{WS} for Al, Mg and Cu are given in table 2. The potential $V_{ss}(r)$ is terminated at $r = 8$, 10 and 7 a.u. for Al, Mg and Cu respectively because it becomes negligibly small for larger values of r.

The calculated $V_{ss}(r)$ for Al, Mg and Cu are shown in figure 1. The number of nearest neighbours and their positions with respect to octahedral site are also indicated there. We find that Mg is more uniformly packed as compared to Al and Cu. $V_{ss}(r)$ has the maxima around the nearest neighbour sites and minima between the two sites. It does not show exact periodicity of the lattice, therefore it can be regarded just as a correction term for the discrete nature of the lattice in $V(r)$ in (4). The potentials depend on Z_H and r_c, however their relative magnitudes are affected by the convergence correction term $3r_c^2/2r_s^3$. This is the reason that magnitude of $V_{ss}(r)$ for Cu and Mg is smaller than that for Al. Thus the discrete lattice effects become more dominant in Al than in Mg and Cu.

3.3 *Phase shifts and impurity potential*

The procedure due to Manninen *et al* [12] is used to solve eqs (3) to (9) self-consistently. The bound states are also included. The radial part of the Schrödinger equation is solved numerically in the steps of 0·1 a.u. up to a radius $R_0 = 19{\cdot}5$ a.u. using Fox

Table 2. The host parameters used in the calculations. r_s is the inter-electronic distance, Z_H is the ionicity, r_c is Ashcroft potential parameter, χ_e is the electronic susceptibility and α_{EW} is Modelung constant for octahedral site. The coordinates of the octahedral sites are given in the last row.

Parameter	Al	Mg	Cu
r_s	2·07	2·66	2·67
Z_H	3	2	1
r_c	1·12	1·39	0·81
$\chi_e(\times 10^{-6})$	1·77	1·58	1·36
α_{EW}	0·42586	0·42732	0·42586
Oct. site	$\left(\frac{1}{2},\frac{1}{2},\frac{1}{2}\right)$	$\left(-\frac{1}{3},\frac{2}{3},\frac{\bar{1}}{3},\frac{1}{4}\right)$	$\left(\frac{1}{2},\frac{1}{2},\frac{1}{2}\right)$

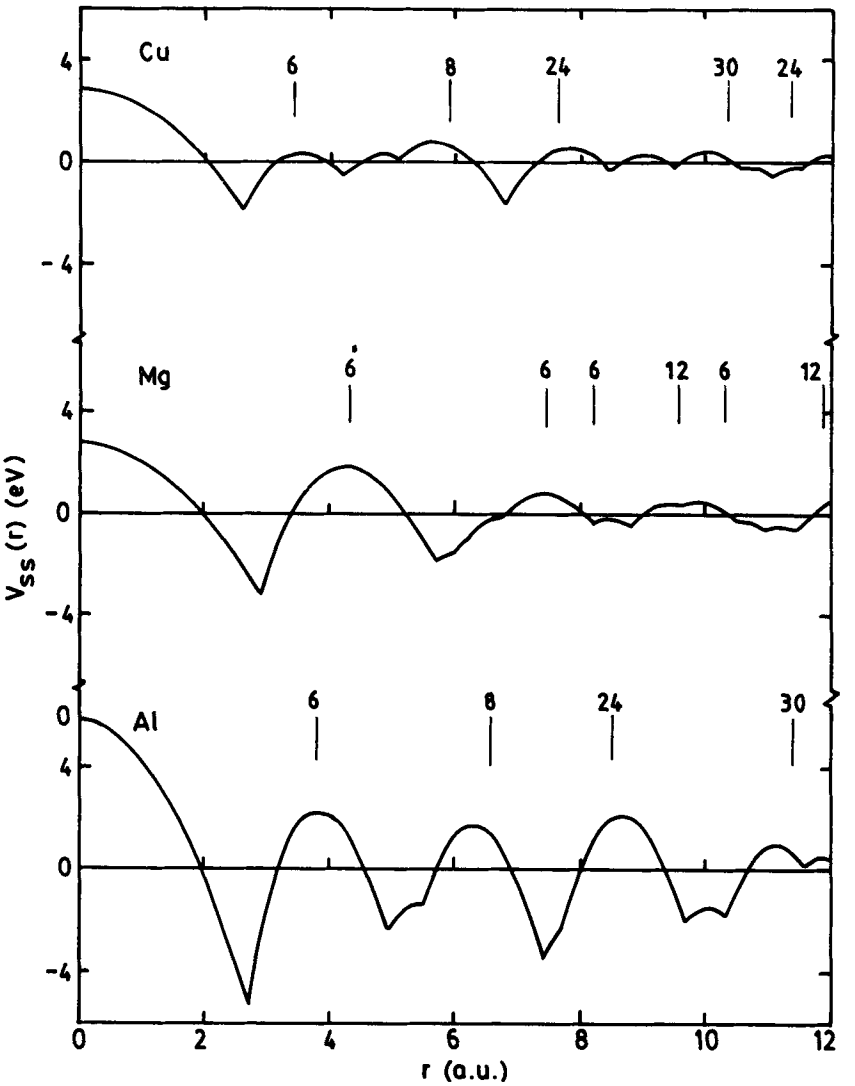

Figure 1. The spherical solid potential $V_{ss}(r)$ vs r for Al, Mg and Cu around octahedral site. The position and number of nearest neighbours are also indicated.

and Goodwin VI method. The phase shifts are calculated by matching the numerical solution with the asymptotic solution at R_0. The self-consistency is checked by satisfying the Friedel sum rule

$$Z = \frac{2}{\pi} \sum_{l=0}^{14} (2l+1)\delta_l(E_F) \tag{18}$$

where l is an orbital quantum number and $\delta_l(E_F)$ are scattering phase shifts at the Fermi energy E_F. The phase shifts are summed up to $l = 14$. Higher order shifts are found negligibly small. The charge density is found accurate within 0·01% in the vicinity of the impurity.

In the first step the calculations are done for the perfect crystal by putting $n(r) = n_H(r)$, $Z = 0$ and $\delta n(r) = n_H(r) - n_0$ in (6), (7) and (18). The self-consistently calculated $V_H(r)$

Table 3. The scattering phase shifts $\delta_l(E_F)$ for proton (H^+) and muon (μ^+) in Al, Mg and Cu. $l = 0, 1, 2...$ are $s, p, d...$ phase shifts

δ_l	Al		Mg		Cu	
	H^+	μ^+	H^+	μ^+	H^+	μ^+
δ_0	0·4646	0·3521	0·6968	0·5760	0·7623	0·6639
δ_1	0·1429	0·1248	0·0454	0·0281	0·1319	0·1255
δ_2	0·0660	0·0628	0·0077	0·0056	−0·0249	−0·0260
δ_3	−0·0614	−0·0619	0·0284	0·0280	0·0174	0·0172
δ_4	−0·0125	−0·0125	0·0008	0·0008	0·0137	0·0136
δ_5	0·0544	0·0545	−0·0044	−0·0044	−0·0008	−0·0009
δ_6	0·0286	0·0287	−0·0027	−0·0027	−0·0025	−0·0025
δ_7	−0·0023	−0·0023	−0·0011	−0·0011	−0·0009	−0·0009
δ_8	−0·0065	−0·0064	−0·0003	−0·0003	−0·0002	−0·0002
δ_9	−0·0030	−0·0030	0·0000	0·0000	0·0000	0·0000
δ_{10}	−0·0008	−0·0008	0·0000	0·0000	0·0000	0·0000

and $\delta n_H(r)$ are obtained. In the next step the calculations are repeated with impurity at the octahedral site by putting $n(r) = n_I(r)$, $\delta n_I(r) = n_I(r) - n_0$ in (6), (7) and (18). The self-consistently calculated $V_I(r)$ and $\delta n_I(r)$ are obtained. The differences

$$\delta V_i(r) = V_I(r) - V_H(r), \tag{19}$$

$$\delta n_i(r) = \delta n_I(r) - \delta n_H(r), \tag{20}$$

give the impurity interaction potential and impurity induced charge density respectively.

The phase shifts which satisfy (18) are tabulated in table 3 for AlH(μ^+), MgH(μ^+) and CuH(μ^+). The s and p phase shifts are leading. The magnitude of higher order phase shifts is oscillatory. Their signs also change and these are slowly converging. This is due to $V_{ss}(r)$ in $V(r)$. We also calculated the phase shifts without $V_{ss}(r)$ (not shown in the table), the magnitudes of phase shifts are reduced by an order of magnitude and rapidly decreasing [5]. Therefore $V_{ss}(r)$ changes the scattering character of impurity at Fermi surface. The size effect is found to reduce the magnitudes of the phase shifts. A relative comparison shows that s phase shifts in Al, Mg and Cu are in increasing order while higher order phase shifts do not show such a trend. The phase shifts converge slowly in Al and faster in Mg and Cu. Thus scattering is more prominent in denser than in rarer electronic medium. The lattice effects are also larger in Al than in Mg and Cu.

The bound states of proton and muon are not found in any of these metals. This is in agreement with the experimental information on the μ^+ in Cu [13]. If the size effect is ignored ($Z = 1$) the shallow s type bound states of energy −0·007 a.u. and −0·0026 a.u. are found in Cu and Mg respectively. However bound state is not favoured in Al due to predominant scattering.

The impurity potentials $\delta V_i(r)$ for AlH(μ^+), MgH(μ^+) and CuH(μ^+) are shown in figures 2, 3 and 4 respectively. The potentials are strongly attractive in the vicinity of the impurity and consists of Friedel oscillations at large distance. A comparison with $\delta V_i(r)$ without $V_{ss}(r)$ [5] shows that the magnitude of maxima and minima is reduced. This is essentially the lattice effect. A relative comparison shows that the magnitudes of $\delta V_i(r)$ in Al, Mg and Cu are in the increasing order. The Ashcroft

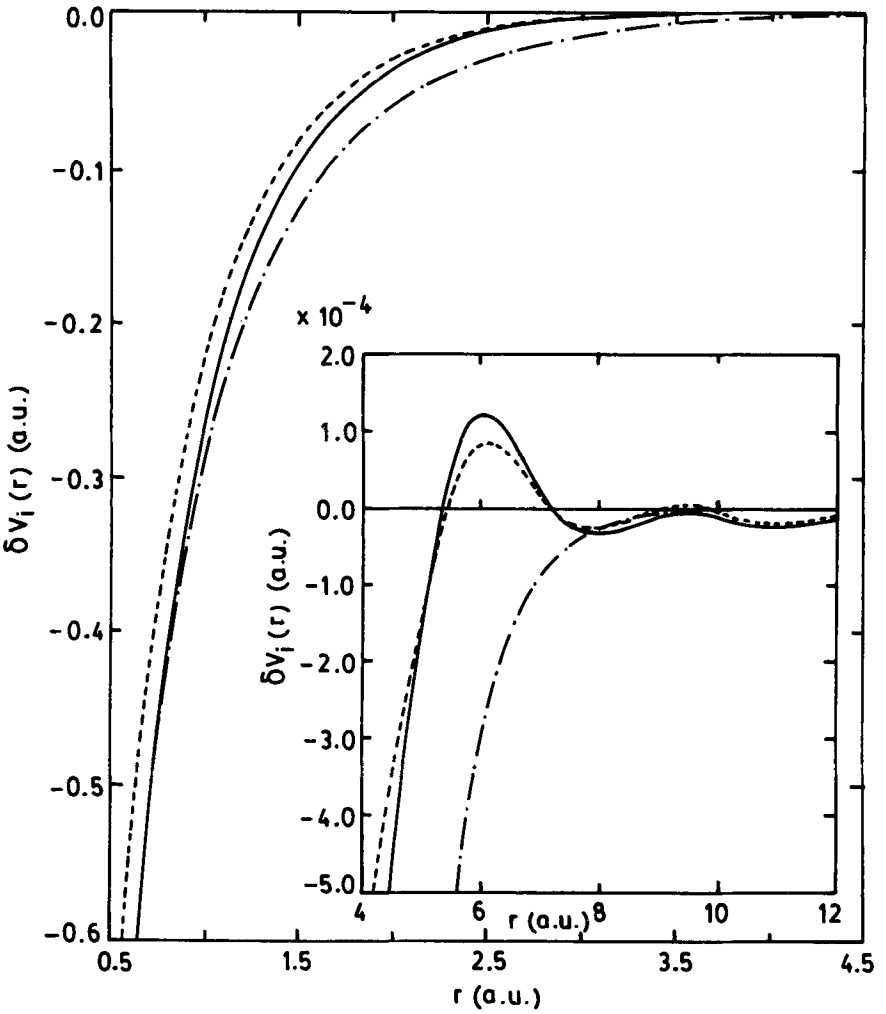

Figure 2. The proton and muon induced self-consistent potential $\delta V_i(r)$ vs r in Al. The solid line represents $\delta V_i(r)$ for proton and dashed line for μ^+. The dash-dot line shows $\delta V_i(r)$ given by equation (21) for proton.

model potential is nonunique within the radius of sphere r_c around each ion. Therefore $\delta V_i(r)$ is found very sensitive to r_c although it explicitly depends on other parameters Z, Z_H and r_s. If the Ashcroft potential is replaced by a more approriate potential $\delta V_i(r)$ will change.

Popovic *et al* [2] suggested the parametrized screened Coulomb potential i.e. $\delta V_i(r) = (-Z/r)\exp(-\alpha' r^{\beta'})$ for hydrogen in metal. α' and β' are determined by satisfying the Friedel sum rule. α' is found in general greater than unity. Sholl and Smith [14] suggested an improved one parameter potential which consists of screened Coulomb term and an exponential term i.e.

$$\delta V_i(r) = -Z\left(1+\frac{\beta r}{2}\right)\frac{\exp(-\beta r)}{r}. \tag{21}$$

This potential is long-ranged as compared to Popovic potential and gives an exact

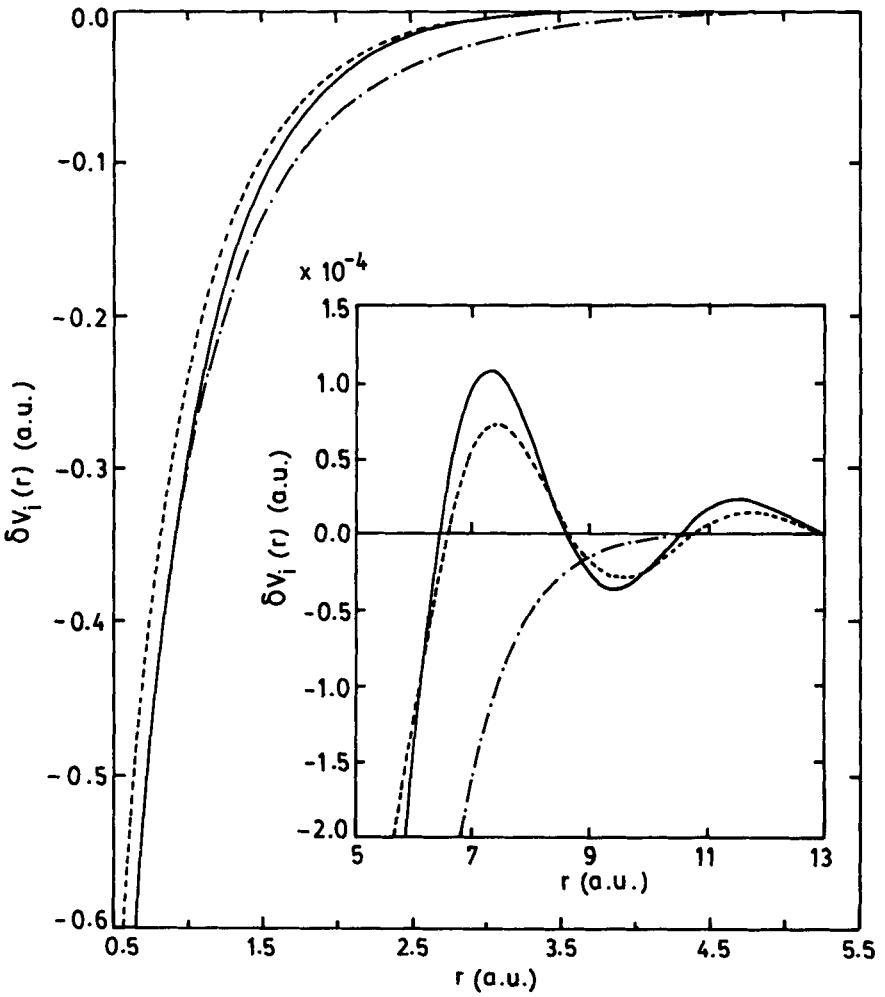

Figure 3. The proton and muon induced self-consistent potential $\delta V_i(r)$ vs r in Mg. The description is the same as that of figure 2.

solution of Poission equation for charge density i.e.

$$\delta n_i(r) = \frac{Z\beta^3}{8\pi} \exp(-\beta r), \tag{22}$$

Equations (21) and (22) are used to describe hydrogen impurity in both the electron gas and transition metals [14]. Therefore we represented our self-consistently calculated $\delta V_i(r)$ in the form of eq. (21) using the method of least square fit. The estimated values of β are given in table 1. For comparison $\delta V_i(r)$ of (21) is also shown in figures 2, 3 and 4. Equation (21) is in good agreement with the self-consistently calculated $\delta V_i(r)$ for smaller value of **r**, however at larger r (21) decreases rapidly while self-consistent $\delta V_i(r)$ is oscillatory. Therefore (21) is quite useful to investigate the short-ranged properties of the impurity.

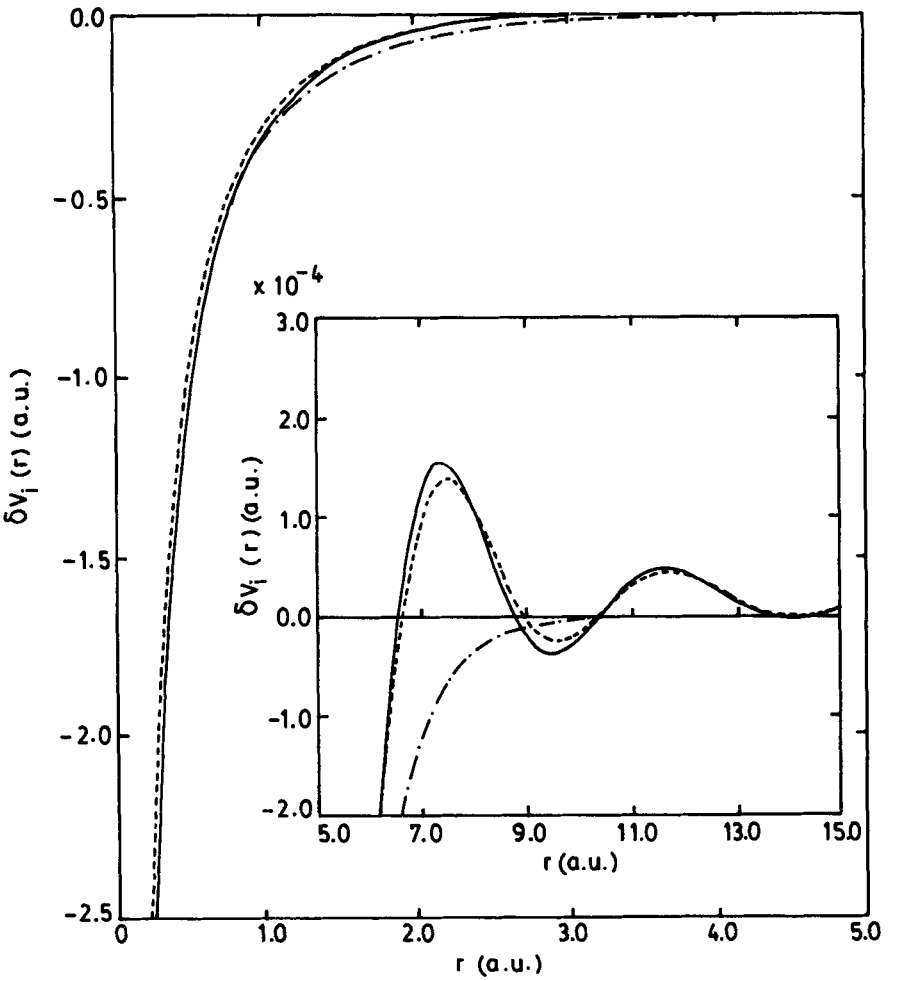

Figure 4. The proton and muon induced self-consistent potential $\delta V_i(r)$ vs r in Cu. The description is the same as that of figure 2.

3.4 *Electronic charge density and charge transfer*

The impurity induced charge density $\delta n_i(r)$ calculated using (20) in Al, Mg and Cu is shown in figures 5, 6 and 7 respectively. There is a pile up of charge on the impurity sites and it decreases rapidly with the increase of r and becomes oscillatory at large r. The charge density in the vicinity of proton is larger than in the vicinity of muon because of larger effective charge on the proton in all the metals. As compared to $\delta n_i(r)$ in jellium model [5] we found that the lattice effect and the size effect both reduce the magnitude of $\delta n_i(r)$. The positions of maxima and minima of $\delta n_i(r)$ also shift due to lattice scattering effects. The charge density given in eq. (22) is finite at the origin and is found smaller than the self-consistently calculated $\delta n_i(r)$.

Using eqs (21) and (22) the impurity induced self-energy is given as

$$E_s = \frac{1}{2}\int \delta V_i(r)\delta n_i(r)\mathrm{d}r$$
$$= \frac{-3}{32}Z^2\beta. \tag{23}$$

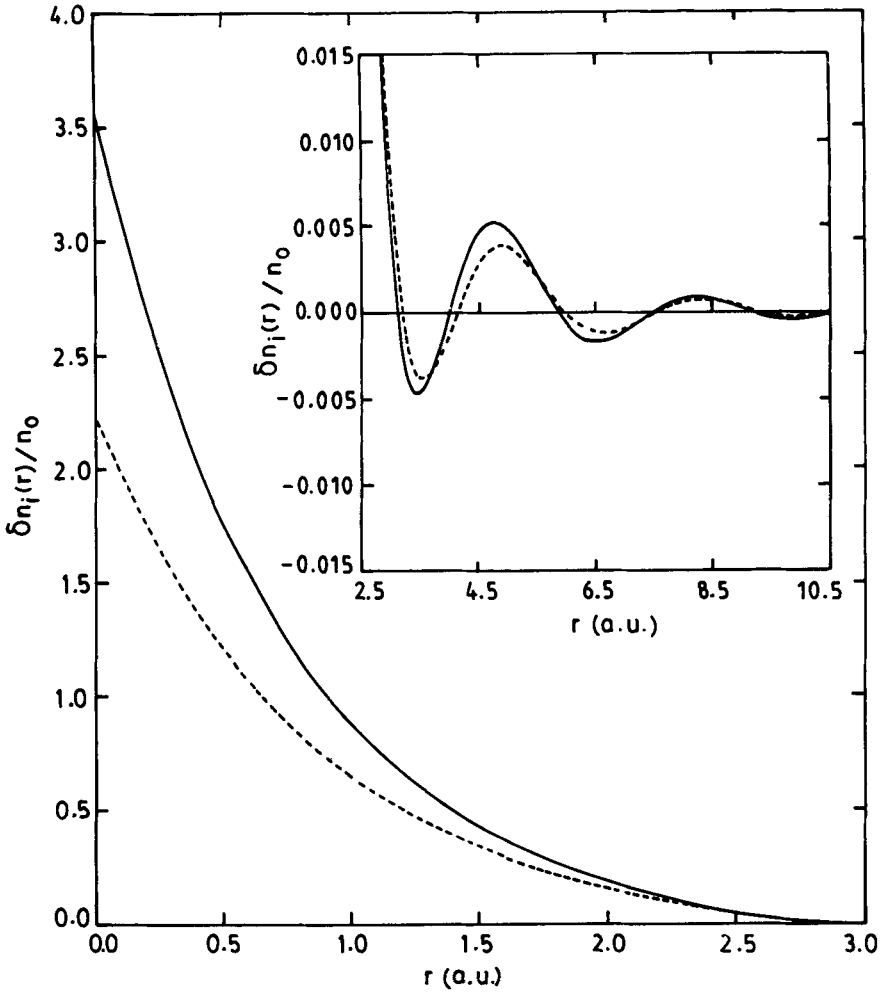

Figure 5. The proton and muon induced change in electronic charge density $\delta n_i(r)/n_0$ vs r in Al. The solid line represents the results for proton and the dashed line for muon.

The calculated E_s for AlH(μ^+), MgH(μ^+) and CuH(μ^+) are tabulated in table 1. The self-energies of proton and muon in Al, Mg and Cu are in increasing order. This is due to the same character of $\delta V_i(r)$ and $\delta n_i(r)$ in these metals. Here E_s can be regarded as lower bound because $\delta n_i(r)$ is underestimated.

The electron charge density $\delta n_i(r)$ is integrated in the hydrogen and muon core radii (1 a.u.) and subtracted from the respective Z values. This gives the net protonic and muonic charges n_s which are also tabulated in table 1. The net charge on proton (muon) is 0·46e (0·39e), 0·45e (0·37e) and 0·54e (0·49e) in Al, Mg and Cu respectively. Thus the virtual bound states are favoured for proton and muon in these metals. The protonic and muonic charges in Cu are in agreement with the earlier calculations of Prakash [15] and Teichler [16]. Comparing with the results of Mahajan and Prakash in jellium model [5] we find that the lattice effects reduce the net charges on proton and muon due to enhanced scattering.

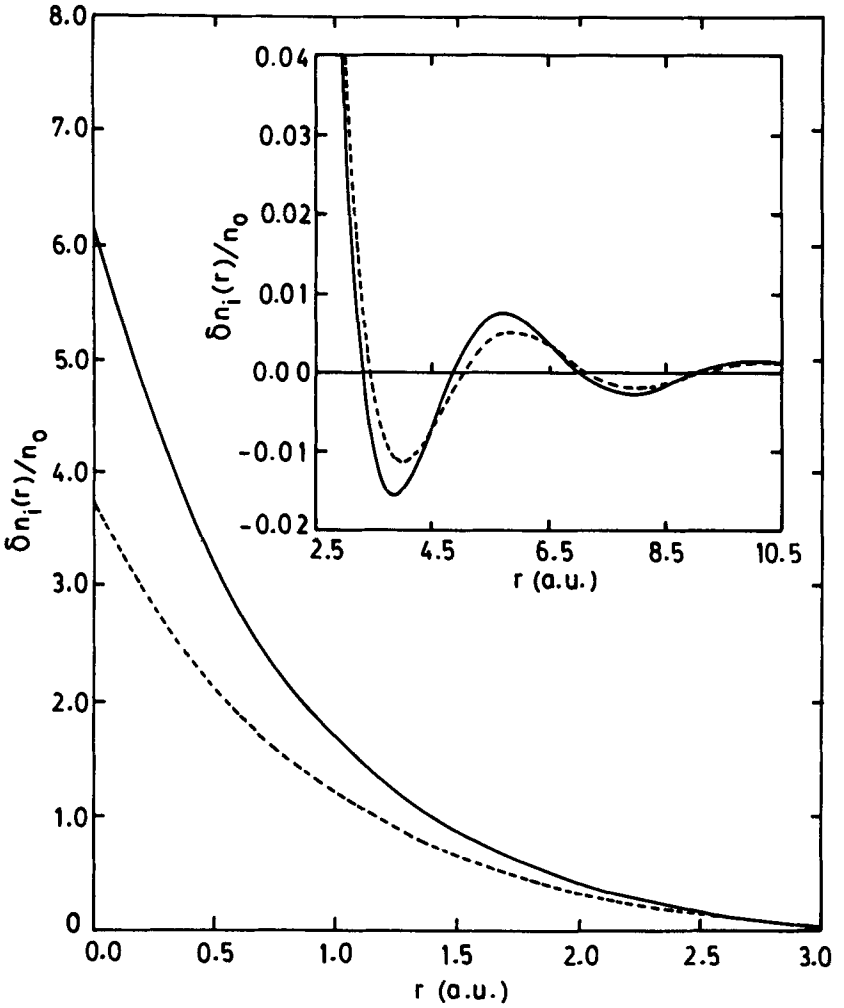

Figure 6. The proton and muon induced change in electronic charge density $\delta n_i(r)/n_0$ vs r in Mg. The description is the same as that of figure 5.

3.5 *Residual resistivity*

The residual resistivity $\Delta\rho$ for AlH(μ^+), MgH(μ^+) and CuH(μ^+) is estimated using expression [1]:

$$\Delta\rho = \frac{2{\cdot}732}{k_F Z_H} \sum_{l=0}^{14} (l+1)\sin^2(\delta_l - \delta_{l+1}). \tag{24}$$

The phase shifts given in table 3 are used.

These calculated values are given in table 1. The residual resistivity for CuH is in agreement with the experimental value [17]. The results for AlH(μ^+) and MgH(μ^+) may be used for further investigations. The resistivity enhances from 5% to 25% if lattice effect $V_{ss}(r)$ is not included. Thus both the size and lattice effects are required to give the correct description of resistivity of these dilute metal hydrides.

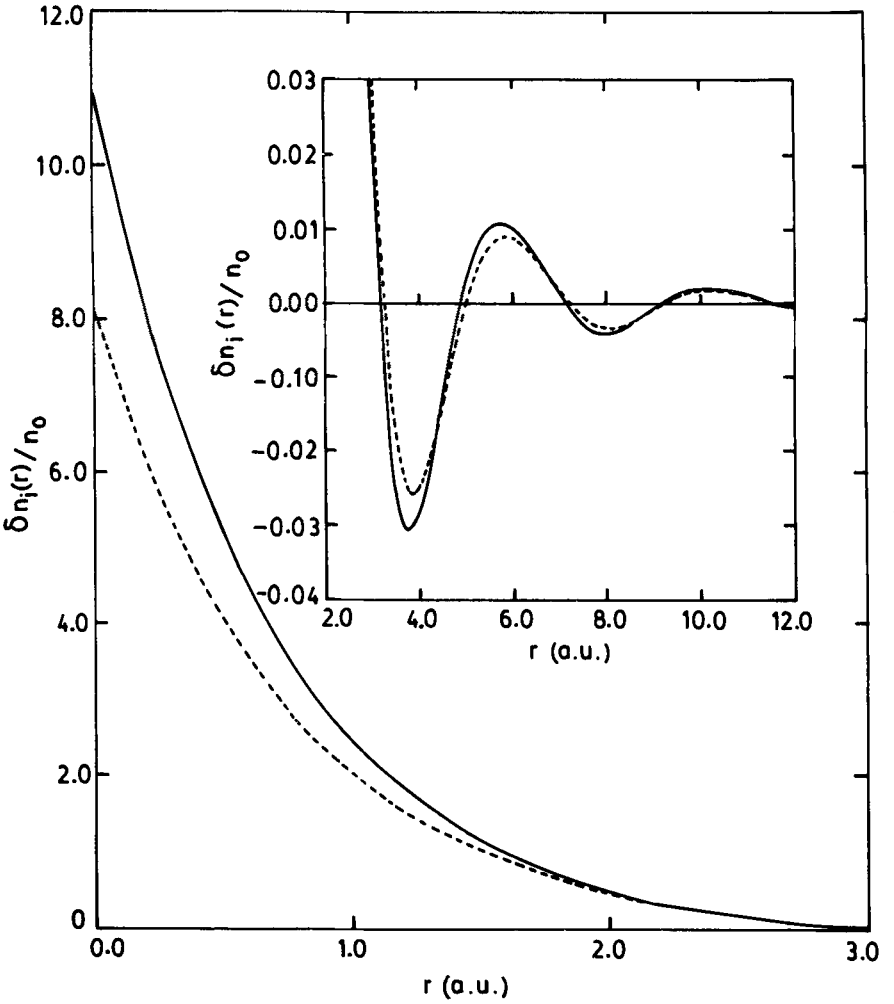

Figure 7. The proton and muon induced change in electronic charge density $\delta n_i(r)/n_0$ vs r in Cu. The description is the same as that of figure 5.

3.6 *Knight shift*

In eq. (4) $V(r)$ is spherically symmetric. Therefore, the Knight shift (the ratio between hyperfine field and the external magnetic field) can be written as the sum of three contributions i.e. [18]

$$K = K_c + K_d + K_z. \tag{25}$$

K_c is Fermi contact term and arises due to the presence of conduction electrons. K_d arises due to the diamagnetic shielding and accounts for the presence of other ions or the positive charge background. K_z is due to zero point motion of the impurity.

It is shown by Mishra *et al* [19] that K_d is smaller by an order of magnitude as compared to K_c and K_z is about 10% of K_c [18]. The proton and muon also do not have the core structure. Therefore the major contribution to K is expected from the

Fermi contact term which is given as

$$K \simeq K_c = \frac{8\pi}{3}\chi_e \frac{n_\uparrow(r) - n_\downarrow(r)}{n_{0\uparrow} - n_{0\downarrow}} \tag{26}$$

where χ_e is the electronic spin susceptibility, $n_\uparrow(r)$ and $n_\downarrow(r)$ are the spin up and spin down electronic densities at the muon site and $n_{0\uparrow}$ and $n_{0\downarrow}$ are the corresponding unperturbed background densities.

To calculate $n_\uparrow(r)$ and $n_\downarrow(r)$, eq. (3) is rewritten as

$$\left[-\frac{1}{2}\nabla^2 + V^\sigma(n, \zeta, \mathbf{r})\right]\psi_{i\sigma}(\mathbf{r}) = \varepsilon_{i\sigma}\psi_{i\sigma}(\mathbf{r}) \tag{27}$$

where the spin dependent potential

$$V^\sigma(n, \zeta, \mathbf{r}) = V_c(\mathbf{r}) + V_{xc}^\sigma(n, \zeta, \mathbf{r}) + V_{ss}(\mathbf{r}) \tag{28}$$

and the spin polarization parameters

$$\zeta(\mathbf{r}) = [n_\uparrow(\mathbf{r}) - n_\downarrow(\mathbf{r})]/[n_\uparrow(\mathbf{r}) + n_\downarrow(\mathbf{r})] \tag{29}$$

and

$$\zeta_0 = (n_{0\uparrow} - n_{0\downarrow})/n_0. \tag{30}$$

The procedure due to Manninen *et al* [4] is used for numerical solution of (27). $\zeta_0 = 0.05$ and the analytical expression for spin dependent exchange-correlation potential $V_{xc}^\sigma(n, \zeta, r)$ due to Gunnarson and Lundqvist [20] are used.

In the first iteration of the solution of (27) the spin independent $V(r)$ is used. $n_\uparrow(\mathbf{r})$ and $n_\downarrow(\mathbf{r})$ are calculated by summing over the allowed states in eq. (6) up to $E_{F\uparrow}$ and $E_{F\downarrow}$ which are determined by the relation

$$E_F\uparrow(\downarrow) = k_F^2\uparrow(\downarrow)/2 \tag{31}$$

where

$$k_{F\uparrow} = (1 + \zeta_0)^{1/3}(9\pi/4)^{1/3}(1/r_s) \tag{32}$$

and $k_{F\downarrow}$ is obtained replacing $(1 + \zeta_0)$ by $(1 - \zeta_0)$ in (32). These values of $n_\uparrow(\mathbf{r})$ and $n_\downarrow(\mathbf{r})$ are used in (29) to determine $\zeta(r)$ and hence the $V^\sigma(n, \zeta, r)$ which is explicity used in later iterations in the self-consistent calculation. $n_\uparrow(\mathbf{r})$ and $n_\downarrow(\mathbf{r})$ are calculated separately and the Friedel sum rule is satisfied by adding the phase shifts for both the calculations i.e.

$$Z = \sum_\sigma Z^\sigma = \frac{2}{\pi}\sum_\sigma \sum_l (2l + 1)\eta_l^\sigma(E_F^\sigma). \tag{33}$$

These values of $n_\uparrow(r)$ and $n_\downarrow(r)$ are used in (26). $(n_{0\uparrow} - n_{0\downarrow})$ is taken from (30) and χ_e from the tabulation of Gygax *et al* [21]. The calculated values of K_c are further enhanced by 10% for zero point motion correction. These final values of Knight shift are tabulated in table 1. The experimental values [20] are also tabulated there.

The calculated values of Knight shift are consistently lower than the experimental values. In the present calculations the size effect is included in the elastic continuum model of the lattice. If the size effect is ignored the calculated radius are 88·96, 112·42 and 92·93 (ppm) for μ^+ in Al, Mg and Cu respectively. These values are consistently

higher than the experimental values. Therefore we conclude that the size effect is important in the determination of the Knight shift. The size effect is known accurately for μ^+ in Cu [11] therefore calculated K is closer to the experimental value for $\underline{\text{Cu}}\mu^+$. The deviation is larger for $\underline{\text{Mg}}\mu^+$ and $\underline{\text{Al}}\mu^+$ as the size effect is just an extrapolated one. It is also noted that K is very sensitive to potential parameter r_c. If r_c is decreased by about 0·2 a.u., the calculated K agrees with the experimental values for Mg and Cu. A small change in r_c and size parameter can bring the calculated K in agreement with the experimental values. Such an attempt is not made in the present calculations as uncertainties are there in χ_e too and $V_{ss}(r)$ is also an approximate lattice potential.

4. Discussion

In these investigations of hydrogen and muonium in monovalent to trivalent metals the detailed electronic structure of metals is not considered. Only the spherically symmetric part of the periodic potential is included. The Fermi surface is assumed essentially spherical and conduction electron wave functions are taken as free particle like. These approximations are reasonable for Al and Mg but may not be justified for Cu as its energy band consists of narrow d-band below Fermi energy. A careful calculation by KKR-Green function method [22] may provide more information. However these involve heavy computational efforts.

The bound states and delocalized states are treated on the same footing using the same one particle potential and exchange-correlation potential. However these potentials may be different for these states. The use of different potentials may require supplementary renormalization procedure which will make the problem intractable.

In conclusion the non-linearity of screening of light impurities in simple metals is fully exploited. Although the discrete lattice and relaxation effects are included in an approximate manner, these effects alter significantly the effective charge, charge transfer, self-energy, residual resistivity and Knight shift of these impurities. The results agree with the experimental values whereever available.

Acknowledgements

The authors acknowledge financial support from the Department of Atomic Energy, Bombay. The authors are thankful to Dr S Mahajan for his help in the calculations of non-linear screening.

References

[1] J Friedel, *Philos. Mag.* **43**, 153 (1952)
[2] Z D Popovic, M J Stott, J P Carbotte and G R Piercy, *Phys. Rev.* **B13**, 590 (1976)
[3] P Jena and K S Singwi, *Phys. Rev.* **B17**, 3518 (1978)
[4] M Manninen and R M Nieminen, *J. Phys.* **F9** 1333 (1979)
[5] S Mahajan and S Prakash, *Nuovo Cimento* **2D**, 883 (1983)
[6] S Mahajan and S Prakash, *Phys. Status Solidi* (*b*) **126** 467 (1984)
[7] W Kohn and L J Sham, *Phys. Rev.* **A140**, 1133 (1965)
[8] P Vashishta and K S Singwi, *Phys. Rev.* **B6**, 8756 (1972)
[9] L Katz, M Guinan and R J Borg, *Phys. Rev.* **B4**, 330 (1971)
[10] R A Oriani, in *Phase stability in metals and alloys*, edited by P S Rudman, J Stringer and R J Jaffe (New York) (1967)

[11] H Schilling, M Camani, F N Gygax, W Ruegg and A Schenck, *Hyperfine Int.* **8**, 675 (1981)
[12] M Manninen, R Nieminen, P Hautojärvi and J Arponen, *Phys. Rev.* **B12**, 4012 (1975)
[13] V G Grvebinnik, *JETP Lett.* **23**, 8 (1976)
[14] C A Sholl and P V Smith, *J. Phys.* **F8**, 775 (1978)
[15] S Prakash, *Phys. Rev.* **B18**, 3980 (1978);
S Prakash, J E Bonnet and P Lucasson, *Phys. Rev.* **B19**, 1976 (1979)
[16] H Teichler, *Phys. Lett.* **A67**, 313 (1978)
[17] R W Wampler and B Lengeler, *Phys. Rev.* **B15**, 4614 (1983)
[18] M Manninen, *Phys. Rev.* **B27**, 53 (1983)
[19] B Mishra, L K Das, T Sahu, G S Tripathi and P K Mishra, *Phys. Lett.* **A106**, 81 (1984)
[20] O Gunnarsson and B I Lundqvist, *Phys. Rev.* **B13**, 4274 (1976)
[21] F N Gygax, A Hinterman, W Rüegg, W A Schenck, W Studer and A J Van der wal, *J. Less Comm. Metals.* **101**, 97 (1984)
[22] J Deutz, P H Dederichs and R Zeller, *J. Phys.* **F11**, 1787 (1981)